

## **Power spectrum characteristics of physiologic and pathologic tremor**

NECIP BERME, ELENA OGGERO, GUIDO PAGNACCO

Mechanical Engineering Dept., The Ohio State University, Columbus OH, U.S.A.

To measure tremor characteristics independently of the testing protocol used (subject standing, sitting, or laying), a highly sensitive ballistocardiographic bed was built using strain gauge technology. This resulted in an accurate, low cost, simple, lightweight and transportable instrument. Coupling this instrument with a high-resolution data acquisition and analysis technique, it was possible to detect the variation in the ground reaction force due to the heart pumping action, and identify its characteristic power spectrum signature. Different experimental protocols were completed, focusing on the inter-subject as well as intra-subject variability, on the gender dependency, on the effect of footwear, on the body and foot position in normal subjects. Furthermore, a preliminary study on tremor inducing pathologies allowed detecting what seems to be a characteristic signature to identify specific tremor aetiology.

*Keywords: tremor measurement*

### **1. Introduction**

Tremor is a poorly understood phenomenon, generally defined as a rhythmical, involuntary, visible oscillatory movement of a body part [1]. Its classification is still inexact, and the most common method of observing and quantifying tremor is subjective in nature, involving the knowledge obtained from the patient about tremor's origin and characteristics, its observation by neurologists, and their assigning a value to the severity based on previous experience.

Recent advancements in the computing power and availability of personal computers allowed for a wide range of techniques to analyse tremor: waveform data, if available, can be analysed to provide useful amplitude or power information, giving a quantitative measurement of the severity of tremor, as well as frequency content of the waveform. The amplitude or power of the tremor waveform is the single most important measure of the severity of tremor. However, amplitude is usually useless in an etiological diagnostic capacity, as markedly different tremors may exhibit similar amplitude. Spectral power analysis still holds promise in a diagnostic ca-

capacity, since it provides information regarding energy at specific frequency [2]. Due to its time-dependent nature, most waveform analyses of tremor characteristics focus on frequency spectrum information. Although it changes slightly between patients with similar aetiologies, and even within one patient from time to time, the average tremor frequency is the most stable parameter available to be tested [2, 3]. It is also useful in determining the underlying cause of the tremor, since there are general frequency ranges within each aetiology usually falls [2].

One of the primary difficulties in observing and diagnosing tremor is the inability to adequately measure the tremor waveform. Different techniques have been used in the past to quantify tremor, including lightweight accelerometers, EMG, EEG, magnetic and optical systems, video recordings with light/dark contrasts, infrared or ultrasound techniques, and positron emission tomography [2, 4]. These techniques present a combination of disadvantages, including high cost, limited portability, the necessity of installing part of the measuring transducer on the subject, and the possibility of doing only local measurements in the area where the sensor is mounted. Force plates have the potential to overcome these problems, but in the past the limitations imposed on the resolution of the measured forces by the instrument and the acquisition electronics and software have seriously affected the applicability of such technology. Because of these limitations, their use was limited until recently to the analysis of the larger force variations induced by the postural sway [5, 6], rather than the tremor itself.

When investigating the overall physiological tremor using a force measuring system, the subject is instructed to stand on the instrument, with feet some distance apart. However, when investigating the tremor characteristics associated with certain pathologies, the subjects might not be able to stand still without external support for the duration of the data collection. In this case, testing protocols requiring the subject to be seated or supine, as well as a force measuring instrument capable of testing a subject independently of the body position are needed.

To measure tremor characteristics independently of the testing protocol used (subject standing, sitting, or laying), a highly sensitive ballistocardiographic bed was built using strain gauge technology. This resulted in an accurate, low cost, simple, lightweight and transportable instrument. Coupling it with a high resolution data acquisition (software based oversampling technique) and a power spectrum analysis, it was possible to detect the variation in the ground reaction force due to the heart pumping action, one of the causes of the physiologic tremor, and identify its characteristic signature. Different experimental protocols involving normal subjects were completed, focusing on the inter-subject as well as intra-subject variability, on the gender dependency, and on the effects of footwear, body and foot position. Furthermore, a preliminary study on tremor-inducing pathologies allowed detecting what seems to be a characteristic signature to identify specific tremor aetiology.

## 2. Methodology

### 2.1. Six-component ballistocardiographic bed

The ballistocardiographic bed, shown in Fig. 1, was designed with the goals of obtaining an accurate, low cost, simple, lightweight and transportable instrument to measure tremor. Strain gauge technology was used to directly measure the forces generated by the physiologic tremor. The instrument was constructed as a 6-component force plate, with a top plate connected to two-instrumented support beams acting as force transducers. To ensure high stiffness and reduce weight, thus increasing frequency response and portability, the top plate was built as a sandwich of honeycomb and aluminium sheets glued together. To improve the accuracy of the measurements, no mattress or other compliant material was included on the top surface. To allow the use of the instrument in different environments, no support legs were included in the design. The load is transferred directly to the supporting surface through small feet (Fig. 2), one of which is adjustable in height to allow for levelling on a non-perfectly flat surface.

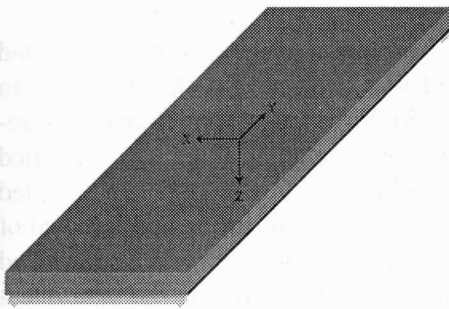


Fig. 1. Ballistocardiographic bed: 3D view

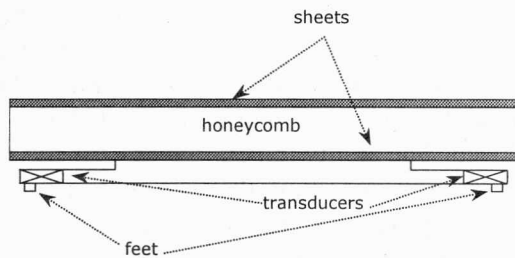


Fig. 2. Ballistocardiographic bed: section view

Two aluminium support beams, rigidly anchored to the top plate, carry at their extremities the force transducers (one for each corner of the instrument). The transducers were designed to be linear up to a maximum deflection due to a load of 2230 N in the vertical direction, and 223 N in the horizontal directions (shears). The strain gauges were positioned so to measure independently the force in the  $x$ ,  $y$ , and  $z$  directions, as identified in Fig. 1. A typical configuration of a complete Wheatstone bridge was used for wiring the gauges with an excitation voltage of 10 V. The analogue signals from each transducer are then conditioned and amplified. The instrument was calibrated using 23 independent loading configurations.

Common testing procedures were followed to assess the characteristics of the new instrument. The bed accuracy was verified by dividing the surface of the instrument in a square grid of 0.1 m, applying a known load (520.537 N) at each grid point and calculating the error both in the load and in its position as measured by the bed. The

accuracy of the shear forces in the  $x$  and  $y$  directions was also evaluated by applying a horizontal load (44.5 N) using a pulley system. The maximum errors in the load components (force and moment along the three axes) and in the positions of the load (in the  $x$  and  $y$  directions and as a vector) are shown in Table 1. The maximum error in the vertical force is 1.09 N when applying a load of 520.537 N, which gives an accuracy of 0.2%. Considering the position of the applied load, the maximum error in the  $x$  direction is 0.0023 m, and in the  $y$  direction is 0.0026 m.

The instrument linearity in the vertical direction, the most susceptible to deformations, was verified loading the bed up to 1010.4 N using ten different calibrated weights and comparing what the instrument measured versus the applied load: in Fig. 3 the points represent the test measurements, whereas the line is the best fit through the same points. Figure 4 illustrates the percent errors in evaluating the linearity of the bed (o-o curve) and the percent errors from the best fitting line (\*-\* curve). The static sensitivity was obtained as the slope of such a curve (0.031 V/N). In the vertical direction, the ballistocardiographic bed is linear in a range from 0 N to 1010.4 N, with an error between the measured and the applied force always less than 2.5%, and less than 0.5% when the bed is loaded with more than 200 N. The decrease in the percentage error is to be expected since the noise, that is almost independent of the loading of the instrument, is relatively more significant with smaller loads.

A specific test was performed to estimate the resolution of the instrument coupled with the signal acquisition chain. First, the bed was preloaded with 520.537 N to simulate a person laying down on it. Then, a 0.0981 N load was applied and then removed. The ability to detect such a small variation in the applied force was estimated by visually inspecting the time plot of the recorded signal. In Figure 5, the sampled data are plotted together with their average to highlight the application and removal of the small force. From the plot, it is possible to detect when the force was first applied and then removed. However, the value of the change was measured by the instrument as being 0.0674 N in loading and 0.0768 N in unloading. This allowed an estimation of the resolution of the instrument in the vertical direction as being approximately 0.03 N, which is approximately the amplitude of the superimposed noise.

Table 1. Maximum absolute errors  
in load and load positioning as measured by the bed

Forces and moments	Centre of pressure
max $ F_x  = 1.38$ N	
max $ F_y  = 0.97$ N	max $ E_{CoPx}  = 0.0023$ m
max $ F_z  = 1.09$ N	max $ E_{CoPy}  = 0.0026$ m
max $ E_{M_x}  = 1.18$ N·m	max $ E_{CoP}  = 0.0029$ m
max $ E_{M_y}  = 1.01$ N·m	
max $ E_{M_z}  = 1.33$ N·m	

The maximum voltage of 5 V that the data acquisition board used could acquire determined the maximum load that could be applied to the instrument before saturation of the acquisition electronics, with a measurement span for the instrument from 0 N to 1645 N.

The frequency response of the bed was investigated exciting the bed in the direction of lower stiffness, the z direction. A steel ball (0.008 m in diameter) was dropped twice in the centre of the top plate and, by spectral analysis, the first natural frequency was estimated at 56 Hz with a damping ratio of 0.008.

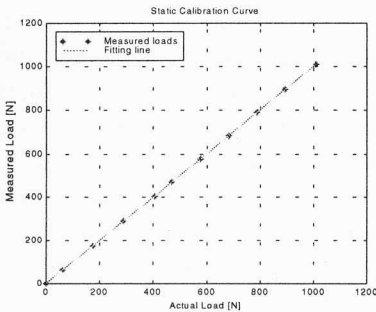


Fig. 3. Linearity of the bed in the z direction

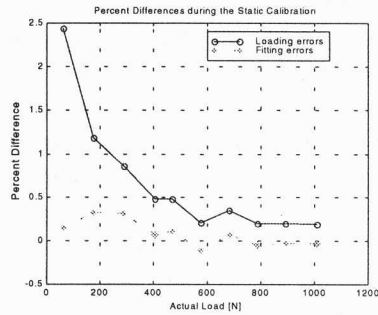


Fig. 4. Percent error in the linearity in the z direction

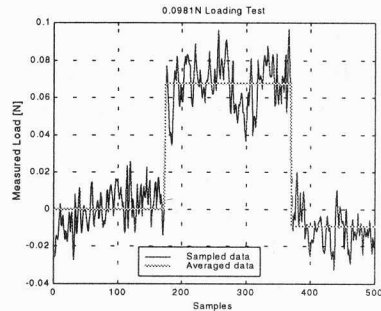


Fig. 5. 0.0981 N loading test of the bed in the z direction

The design choices made for the ballistocardiographic bed allowed the construction of a portable instrument that can be positioned directly on a hard level surface, without requiring any special set up apparatus. This was achieved with the same design philosophy commonly used for force plates: four strain gauge transducers coupled with a rigid structure. This design resulted in an instrument capable of measuring the physiologic tremor in all its components (force and moment along three orthogonal axes). Even if the dimensions of the device are significant in order to accommodate the majority of the subjects, the design choice of the top plate as a honeycomb sandwiched structure yielded a total mass for the entire instrument of only 18 kg

(40 lb.). The results of the mechanical characterisation show that the bed can be considered an accurate instrument and the errors in the measured loads are comparable with what found using standard size force plates.

## 2.2. Software-based oversampling technique

This software-based oversampling technique consists of three steps. First, the analogue signal is sampled at a much higher sampling rate than otherwise required by the frequency content of the signal itself. The ratio between the actual sampling rate and the rate necessary to preserve the frequency information, or the frequency, at which the signal would have been sampled had this technique not been used, is called the oversampling ratio. The digitised signal is then numerically low-pass filtered using double precision arithmetic to reduce the errors introduced by the computations. Finally, if desired, the number of samples can be reduced by downsampling the signal, to produce the same number of samples that would have been collected if this technique were not used. This last step allows limiting the amount of storage required by the resulting data without losing any information.

The digital signal can be seen as the actual analogue signal of interest plus superimposed noise. A reduction of the noise improves the resolution. To understand how the noise can be reduced it is necessary to consider what happens to the signal and the noise during sampling. In particular, it is necessary to understand the concept of aliasing: any time a signal component of frequency higher than half of the sampling rate is digitised, it appears as a component of the same amplitude or power, but lower frequency, as if reflected back (aliased) into the frequency range from zero to half of the sampling rate. The sampling rate is often chosen considering only the analogue signal of interest, and not the noise superimposed on it. For this reason the signal does not suffer from aliasing, whereas the noise, that usually has components at frequencies much higher than the signal, is affected (Fig. 6). If the sampling rate is chosen equal to the Nyquist rate for the signal, then noise and signal are superimposed, and this makes it impossible to reduce the noise, as there is no way to separate it from the signal after sampling occurs. If, however, the sampling rate used is much higher than the Nyquist rate for the signal (i.e., an oversampling is performed), then at least some separation between the signal and the noise is generally possible. In fact, since the total power is unaffected by aliasing, if the noise becomes aliased over a larger frequency range, then its power in the same frequency range of the signal is decreased. Oversampling changes the spectral distribution of the noise and allows a reduction of the noise at the same frequencies of the signal.

The digital signal does not have any more resolution because of the oversampling itself. However, since noise and signal are more spectrally separated, it is now possible to reduce the noise power without affecting the signal. This is done by low-pass filtering the oversampled signal (Fig. 7) using a high-order digital filter specifically designed to minimise the effects on the signal of interest. After the filtering, the

power spectral density at all frequencies higher than the filter cut-off frequency is reduced, and so is the overall power content of the noise. This is in fact the integral of the power spectral density across the frequency domain.

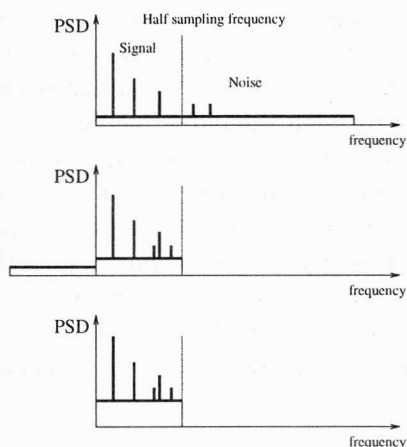


Fig. 6. Qualitative effect of aliasing (see text) on the Power Spectral Density (PSD)

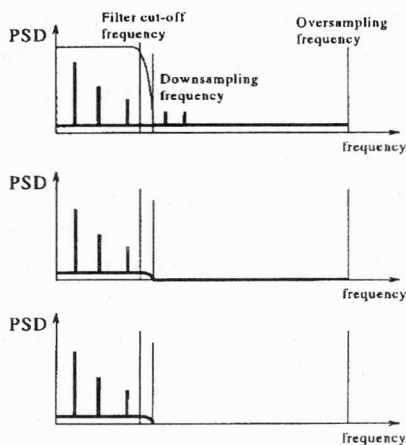


Fig. 7. Qualitative effect of oversampling, filtering, and downsampling of the signal

Since the filtering removes the spectral power content of the higher frequencies, it is possible to re-sample the filtered signal at a lower rate to reduce the number of samples without any loss of information and any adverse aliasing effect. This process is called downsampling and can be performed by simply keeping one sample out of every so many.

Since the noise power of the digital signal obtained by this method is reduced, its Signal to Noise Ratio (SNR, ratio between the signal and the noise power) is increased, and the resolution is improved. In particular, the improvement of the noise power and the SNR is:

$$\frac{\text{Noise}_{\text{Original}}}{\text{Noise}_{\text{Oversampling}}} \tag{1}$$

and the amplitude resolution improvement is its square root:

$$\sqrt{\frac{\text{Noise}_{\text{Original}}}{\text{Noise}_{\text{Oversampling}}}} \tag{2}$$

As these expressions suggest, the improvement is a function of the overall noise spectrum. If the noise is white, and a filter of infinite order is used, then the ratio in Eq. (1) is equal to the oversampling ratio. This can be used to estimate the improvement. If the noise is not white, but most of it is shifted out of the signal frequency range by the oversampling, then the improvement can be even larger. On the other

hand, the improvement can also be less, because the filters used in practice have a high but finite order, and the noise might be largely concentrated in the signal band.

The advantages of this software implemented oversampling technique are improved resolution, reduced need for anti-aliasing filters, reduced errors in the case of insufficiently high sampling frequency, and with some analogue to digital converters reduced time skew error between channels in the case of multichannel acquisitions. These same benefits can otherwise be obtained only by using equipment that is much more expensive. The disadvantages are the need for high sampling rate devices, the large processing storage, and the significant number of computations required by the digital low-pass filtering. Also, there is a need to extend the acquisition before and after the required duration in order to minimise the filter edge effects. In the past, these disadvantages significantly limited the applicability of this technique. Less than a decade ago, it would have been impractical, very expensive, or even impossible. Presently, however, these limitations are of no concern due to the availability of low priced, very fast analogue to digital converters, and fast computers with large amounts of memory.

### 2.3. Tremor power spectrum

The possibility exists that a subject's tremor power spectral density can shift in time. Certain tremors due to neurological disorders are more pronounced during certain voluntary activities (action tremors) [3]. A patient concentrating on standing still may actually change tremor characteristics in the effort to perform well on the test, but may become more relaxed and show less tremor as the testing progresses. Furthermore, the presence of the heartbeat could constitute a possible source of equilibrium perturbation. It is therefore insufficient to perform a single discrete Fourier transform on all the data, since in doing so the timing information is lost and it is not possible to identify when each frequency was present in the tremor. Furthermore, if a shift in frequency is present, it is not possible to identify it since all frequencies present in the signal during the entire duration of the data collection are shown together when using such a transform. Because of this, the data need to be analysed in the phase plane (time-frequency plane) using the short-time Fourier transform (STFT), and the power spectral density estimated using the Welch method [7].

Considering a set of data, a Hanning window is used to isolate a subset of the samples (Fig. 8a). These are then zero-padded to a length of  $2^n$  samples (Fig. 8b) and the discrete Fourier transform is computed, yielding the power spectrum of the subset of data (Fig. 8c). The window is then moved several samples (Fig. 8d) to generate an overlap with the previous window plus the new samples. The analysis procedure is then reapplied on the new subset of data. Once all the subsets of the considered data are analysed, the average of the obtained power spectra is calculated resulting in a typical curve for each set of data (Fig. 9). To avoid dependency of the power spectrum from the used window size and shape, the curve is normalised so that its integral



equals one. This analysis procedure yields to a statistical estimation of the power spectral density of the entire signal, giving for each frequency the corresponding percentage of power.

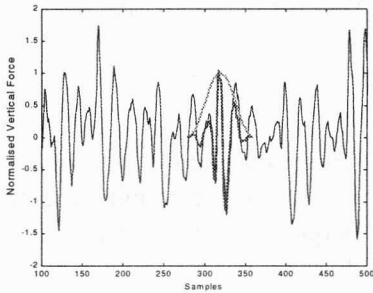


Fig. 8a. Schematics of data analysis: Hanning windows applied to the data

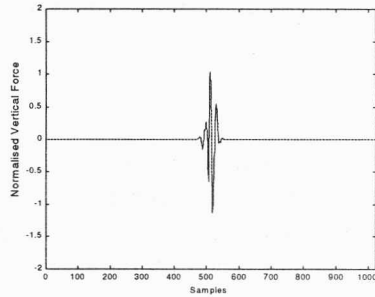


Fig. 8b. Schematics of data analysis: data zero-padded to  $2^n$  (1024 in this case) samples

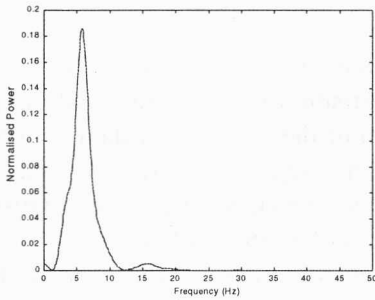


Fig. 8c. Schematics of data analysis: power spectrum of the subset of data

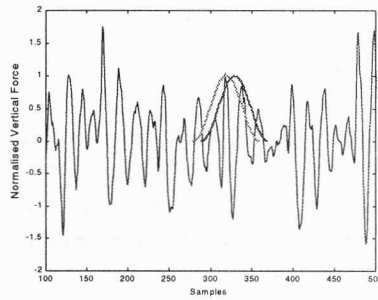


Fig. 8d. Schematics of data analysis: Hanning windows moved several samples

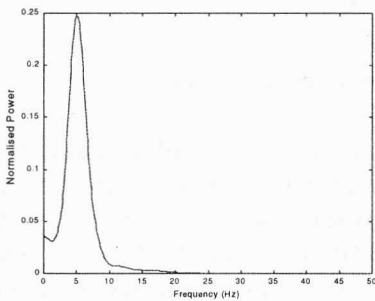


Fig. 9 Example of the power spectrum of an analysed signal

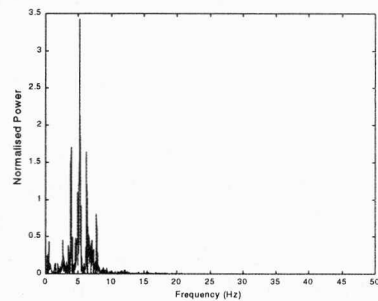


Fig. 10. Power spectrum of the same signal obtained using the Fourier transform

The total energy content of the signal is calculated in the time domain as

$$E_{\text{tot}} = \int A_t^2 dt \quad (3)$$

and then normalised by the acquisition duration  $\Delta t$  to obtain an average total power

$$P_{\text{tot}} = \frac{E_{\text{tot}}}{\Delta t} \quad (4)$$

that allows comparison between tests with different acquisition duration. Furthermore, given Parseval's theorem (the total energy of the signal is independent of the method used to calculate it, in the time or in the frequency domain), this average total power can be multiplied by the power spectrum to yield the effective average power content of the signal at each frequency.

From the power spectrum, the mean frequency  $f_{\text{ave}}$  is calculated [8]:

$$f_{\text{ave}} = \frac{\int f dA}{\int dA} = \int f dA. \quad (5)$$

(Note that the integral under the curve is, by normalisation, equal to one.)

It is possible to appreciate the superior information given by the analysis procedure presented here versus the Fourier transform of the same set of data, by comparing Fig. 9 to Fig. 10. Not only is the detection of a typical spectrum facilitated, but also given the time-varying characteristics of the signal, a much more statistically accurate estimate of the average spectral power distribution is obtained.

From this analysis procedure, three parameters were obtained to characterise the physiological tremor: the mean frequency, the average total power content, and the power spectrum.

### 3. Applications

#### 3.1. Tremor characteristics in normal subjects

Ten subjects, five males, age 22 to 35 (average 26.2, standard deviation 5.4, median 25), and five females, age 20 to 28 (average 21.6, standard deviation 3.6, median 20), participated in this study. All subjects were self-assessed to be in good health, without known neuropathological conditions, and information such as amount of sleep, quantity of caffeine or alcohol consumed, and possible medications were noted, since they are reportedly known to affect the tremor characteristics [3]. The subjects were tested twice over a period of one week. Each subject stood motionless, relaxed, and unsupported on the ballistocardiographic bed for the entire duration of the data

collection. To test the intra-subject repeatability, one subject was tested 20 times over a period of two hours. A total of 60 trials were collected.

As shoes were the only item between the subject and the instrument, each subject performed the tests both with and without them, in order to assess their influence on the tremor characteristics. In this study, shoe types tested were oxfords, tennis shoes, and hiking boots. All contained rubber soles.

The results of the inter-subject analysis are illustrated in Fig. 11, where the average of the power spectra is plotted along with the curves representing the average plus or minus the standard deviation. In the same figure, the average mean frequency (5.54 Hz), and its 95% confidence are shown by the vertical lines. The standard deviation of the mean frequency was found 0.419 Hz. The corridor defined by the average plus or minus the standard deviation of the analysed spectra shows that, whereas an overall typical shape can be qualitatively identified, the magnitude varies significantly between subjects. This is confirmed by the small standard deviation of the mean frequency and the large standard deviation of the amplitude around the peak values.

The results of the intra-subject analysis are similarly illustrated in Fig. 12. The computed average mean frequency was in this case 5.61 Hz, with a standard deviation of 0.397 Hz. There is a good repeatability over time, considering the possible variation of the physiological tremor over a period of two hours, reported in the literature. The observations made about the inter-subject variability can also be applied in this situation. Whereas the variability of the mean frequency is small, the variability of the peak as well as average power is significant. However, it is possible to identify a qualitative shape of the spectrum typical for the subject.

The results for the gender dependency and effect of footwear are similarly illustrated in Figs. 13 and 14, respectively.

The numerical values for the average frequency and its standard deviation and the average total power and its standard deviation for the performed analyses are included in Table 2.

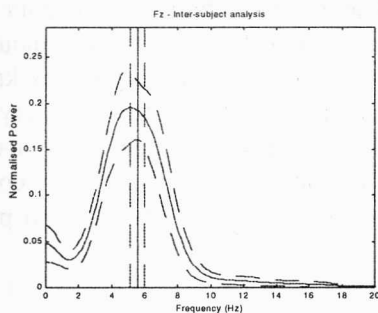


Fig. 11. Power spectrum and mean frequency: inter-subject analysis

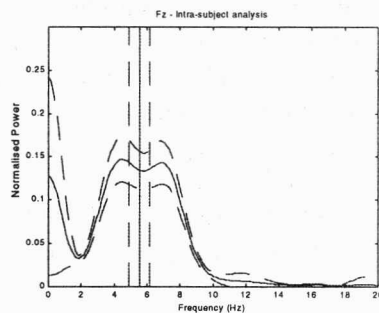


Fig. 12. Power spectrum and mean frequency: intra-subject analysis

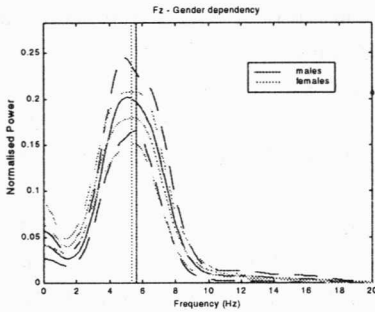


Fig. 13. Power spectrum and mean frequency: gender dependency

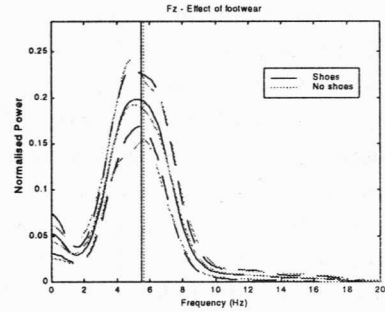


Fig. 14. Power spectrum and mean frequency: effect of footwear

Table 2. Mean value and its standard deviation for the mean frequency and total power for normal subjects

Analysis	Mean frequency [Hz]	Normalised total power
Inter-subject	$5.57 \pm 0.42$	$1.05\text{E-}006 \pm 3.63\text{E-}007$
Infra-subject	$5.53 \pm 0.64$	$1.32\text{E-}006 \pm 2.70\text{E-}007$
Shoes	$5.52 \pm 0.45$	$1.06\text{E-}006 \pm 4.03\text{E-}007$
No shoes	$5.62 \pm 0.40$	$1.03\text{E-}006 \pm 3.32\text{E-}007$
Males	$5.66 \pm 0.39$	$1.18\text{E-}006 \pm 3.38\text{E-}007$
Females	$5.34 \pm 0.41$	$7.19\text{E-}007 \pm 1.63\text{E-}007$

The power spectrum and the mean frequency obtained are repeatable: the inter-subject analysis shows that an overall typical spectrum can be qualitatively identified. As highlighted by the intra-subject analysis, this spectrum does not change over time. Furthermore, the spectrum and the mean frequency do not show a significant dependency on gender or presence of footwear. The average total power appears more subject dependent: this can be explained considering that factors such as amount of sleep, quantity of caffeine consumed, and possible medications are reportedly known to affect the tremor characteristics [3], but the magnitude of their effects is very subject dependent, making quantification difficult. Given the small value of the average total power (in the order of  $10^{-6}$ ), very small fluctuations can change its value considerably, as confirmed by the relevant standard deviation obtained for the total power during the different analyses (Table 2).

### 3.2. Effects of body position

15 subjects, age 23 to 33, participated in this preliminary study. Immediately prior to each test, the subject's blood pressure and pulse rate were recorded. 10 different

body positions (laying on the back, on the left side, on the right side, on the belly, and on the back in a foetal position; sitting with legs crossed, and supported; standing on both feet, on the right foot only, and on the left foot only) were investigated. Data were sampled for 60 s at 48 Hz with an oversampling factor of 64, using a 12-bits data acquisition board. The force in the subject's head-to-toe direction was analysed using the Short Time Fourier transform and the power spectrum was calculated using the Welch method. A statistical analysis was performed to assess the relevance of the position to the tremor spectrum, mean frequency and total power, as well as the inter-subject variability.

Figure 15 shows the power spectrum as a function of the overall body position (laying, sitting, and standing). The curves represent the average power spectrum in the specific body position. In the standing position, only the tests with bipedal support were considered, since the power in the other two cases (standing on one foot only) was more than an order of magnitude larger.

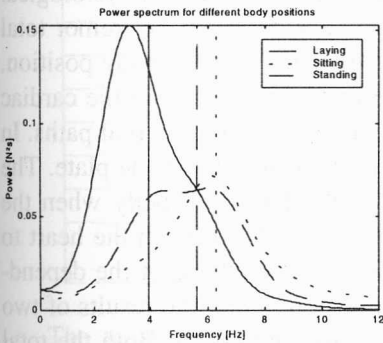


Fig. 15. Physiological power spectrum for different body positions

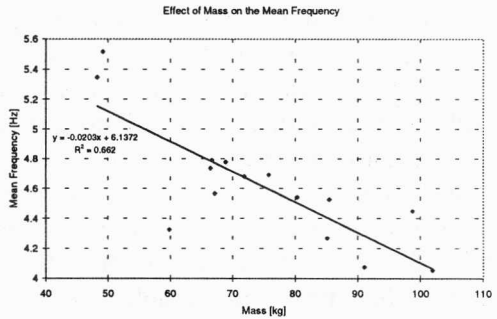


Fig. 16. Effect of subject's mass on mean frequency

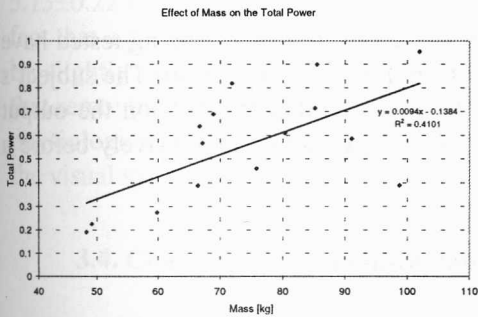


Fig. 17. Effect of subject's mass on total power

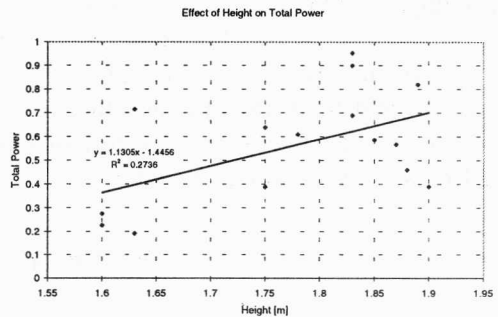


Fig. 18. Effect of subject's height on total power

The preliminary results obtained so far point toward a dependency of the physiological tremor frequency characteristics (power spectrum, mean frequency, and total power content) on the subject's body position. These findings were confirmed with

a significance level of 0.01 by a two-way ANOVA with interaction on the mean frequency and the power spectrum. The heart rate and blood pressure did not appear to be a significant factor, as well as other factors such as subject's age, sex, and percentage of body fat. The total power and mean frequency were however affected by the height and mass of the subject. Figure 16, which depicts the effect of the subject's mass on the mean frequency, reveals that the mean frequency decreases as the mass increases, whereas the height didn't have any significant effect. The total power was affected by both subject's mass and height, as shown in Figures 17 and 18: total power increases as the subject's mass/height increases, as expected since usually an increase in height corresponds to an increase in mass.

These results confirm that the physiological tremor seems to be affected by the heart pumping action. However, a slight shift toward a lower value for the average frequency and toward a higher value for the total power seems to indicate a more complex relationship between the effect of the heart contraction and the physiological tremor. The results suggest that a strong relationship exists between the tremor total power and the body position and between the mean frequency and the body position. When the subject is placed in different positions, the forces generated by the cardiac cycle are transmitted to the ballistocardiographic bed along different internal paths. In some of these positions, the heart is quite far from the actual surface of the plate. The values were maximum for the subject when laying on the back and belly when the heart was closest to the bed surface. This implies that the distance from the heart to the bed seems to be an important factor on the signal. A consequence of the dependency of the ballistocardiographic signal on the body position is that the results of two studies cannot be compared directly unless the same position is used. Both the total power and mean frequency of the ballistocardiographic signal were found to vary with the subject height and mass. The total power of the signal was found to increase for increasing height and mass. These results seem logical because a larger mass of blood is being distributed in larger person.

In addition, it was found that the height and mass of the subject being tested have a significant effect on the total power and mean frequency of the signal. The subject's age, percent body fat, and sex did not seem to have significant effect on the output signal, but these subject characteristics need to be studied more extensively before a definitive conclusion is reached.

### 3.3. Effects of foot position

15 subjects, age 19 to 33, participated in this study to determine the effect of foot position (anteroposterior, mediolateral, and angular) on the tremor spectral characteristics (power spectrum, average frequency, and total power). The dimensions of the considered support ranged from zero to 0.1m in the anteroposterior direction, from zero to 0.2 m in the mediolateral, and from 0° to 60° in the angular position. All study participants were in self-described good health, with no previous diagnosis of neuro-

logic dysfunction and never previously broken a lower extremity. Prior to testing, physical characteristics of pulse rate, blood pressure, temperature, and measurements to determine percentage body fat were obtained and recorded. Ten different positions were used to verify the effect of foot positioning of the tremor parameters (Table 3). Furthermore, the effect of eyes open and closed was also investigated to assess the influence of the visual system on the tremor characteristics while standing.

Table 3. Foot positioning: anteroposterior *Y*, mediolateral *X* and angular theta

<i>X</i> [cm]	<i>Y</i> [cm]	Theta [°]
0	0	0
10	10	0
20	0	0
0	0	30
20	10	0
20	0	60
20	10	60
0	10	60
0	0	60
10	0	60

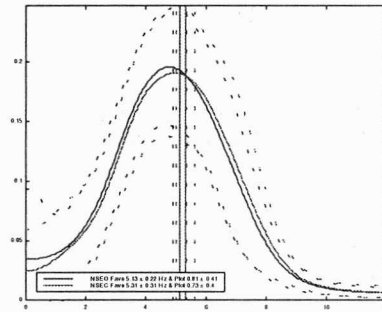


Fig. 19. Average tremor power spectrum across all positions, eyes open and closed

The results obtained could not identify a statistically significant effect on the tremor parameters. The average frequency, total power and power spectrum do not significantly change with changing foot position. Similarly, the effect of the visual stimulus does not affect them as well (the average frequency changed from  $5.13 \pm 0.22$  Hz with eyes open to  $5.31 \pm 0.31$  Hz with eyes closed). This confirms the fact that a physiologic tremor signature exists indeed, and is not affected significantly by slightly changes in the foot position as those investigated. Furthermore, the fact that removing the visual stimulus does not affect the results seems to indicate that the physiologic tremor is not influenced by the balance controlling mechanisms, of which the visual system is part.

### 3.4. Changes in tremor characteristics due to neurological pathologies

Four subjects affected by Parkinson's disease (three males and one female) and nine subjects affected by multiple sclerosis (one male and eight females) were tested, as a preliminary investigation of the differences between the physiological and pathological tremor signature. Their power spectra are shown in Fig. 20 (Parkinsonian patients), and Figs. 21 and 22 (MS patients), and the numerical values for the mean frequency and total power are included in Table 4.

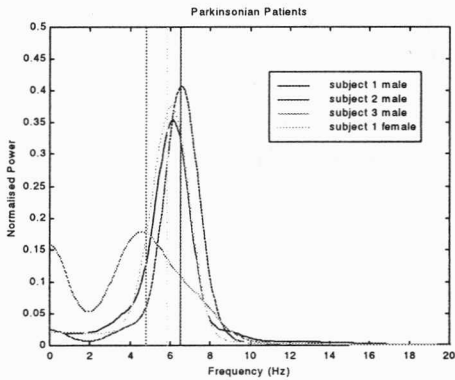


Fig. 20. Power spectrum and mean frequency: Parkinson's disease subjects

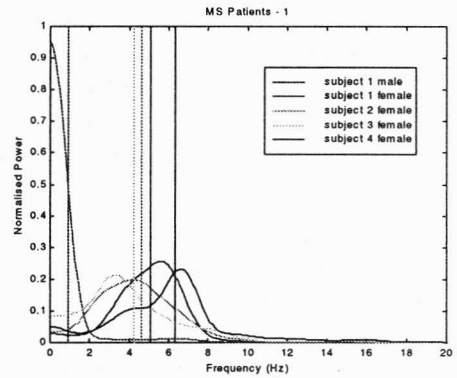


Fig. 21. Power spectrum and mean frequency: multiple sclerosis subjects - 1

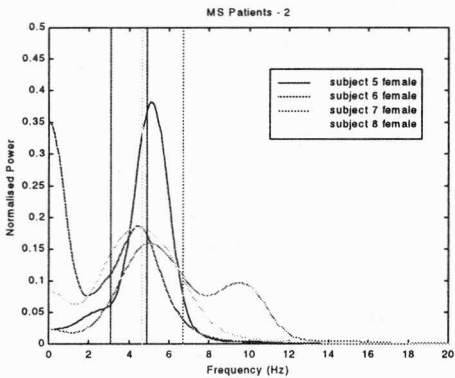


Fig. 22. Power spectrum and mean frequency: multiple sclerosis subjects - 2

Considering these results, it seems possible to identify a characteristic signature of such a pathology: the power spectrum and the mean frequency seems to be correlated with the disease type and progression. A subject affected by Parkinson's disease present a shift toward a higher mean frequency compared to normal subjects, and the shape of the power spectrum is narrower and more concentrated around the mean frequency, with peak values almost double the normal case. On the contrary, a subject affected by multiple sclerosis has the mean frequency shifted toward lower values compared to normal subjects, the more the disease is advanced, the higher the shift. The shape of the power spectrum remains similar to the normal case, but when the subject feels uncomfortable standing still or needs external support to stand for long period of time, the shape of the power spectrum presents a maximum at the zero frequency with values significantly higher than normal (almost 1 in one case, compared



Table 4. Mean frequency and total power for subjects affected by neurologic pathologies

Disease	Subject	Mean frequency [Hz]	Normalised total power
Parkinson's disease	1 male	6,50	2.01E-006
	2 male	6.52	1.64E-006
	3 male	4.81	2.91E-007
	1 female	5.85	3.50E-006
Multiple sclerosis	1 male	5.09	1.10E-006
	1 female	0.95	1.49E-005
	2 female	4.61	1.10E-006
	3 female	4.26	2.31E-006
	4 female	6.31	8.71E-007
	5 female	4.88	4.52E-006
	6 female	3.09	8.11E-005
	7 female	6.72	7.52E-005
8 female	4.66	2.48E-007	

to the normal 0.25). Considering the total power, it is more difficult to identify a characteristic signature for each pathology: again it seems more subject dependent, even more than in the case of normal subjects, given the fact that some subjects were under drug treatment to reduce the tremor symptoms.

#### 4. Conclusions

The results obtained show that it is possible to use force plates in general and a ballistocardiographic bed in particular, to quantify tremor. The advantages can be significant: it is a non-invasive instrument, without the necessity of installing part of the measuring transducer on the subject; it only requires the subject to stand on it; and it is easy to use in any clinical setting given its portability. Furthermore, the high sensitivity of the acquisition technique using oversampling allows detecting the variation induced by the cardiovascular system, even after being filtered by the entire body. The analysis procedure is consistent, repeatable and yields results comparable with what found in the literature using different measurement techniques. It was possible to identify three characteristic parameters for the physiological tremor: the mean frequency, the power spectrum, and the average total power. In particular, the mean frequency and the power spectrum can be used to identify the physiological tremor signature: they are repeatable over time and across subjects, do not show a gender dependency, are not affected by the presence or absence of shoes with rubber soles, and do not depend on the foot position nor on the presence of the visual stimulus. The

average total power is more subject dependent. The measurements of overall body tremor obtained in different postures are not directly comparable: the tremor characteristics for normal subjects in different postures should be obtained as reference for investigating pathological tremor, since they appear to have a characteristic signature that could be potentially used to distinguish between different aetiologies and to monitor the onset of the disease.

### References

- [1] FINDLEY L.J., KOLLER W.C., *Handbook of tremor disorders*, Marcel Dekker, New York, 1995.
- [2] DEUSCHL G., KRACK P., LAUK M., TRIMMER J., *Clinical neurophysiology of tremor*, Journal of clinical neurophysiology, 1996, Vol. 13, No. 2, pp. 110–121.
- [3] FINDLEY L.J., *Classification of tremors*, Journal of clinical neurophysiology, 1996, Vol. 13, No. 2, pp. 122–132.
- [4] BEUTER A., DE GEOFFROY A., CORTO P., *The measurement of tremor using simple lasers system*, Journal of Neuroscience Methods, 1994, Vol. 53, pp. 47–54.
- [5] LE CLAIR K., RIACH C., *Postural stability measures: what to measure and for how long*, Clinical Biomechanics, 1996, Vol. 11, No. 3, pp. 176–178.
- [6] SCHUMANN T., REDFERN M. S., FURMAN J.M., EL-JAROUDI A., CHAPARRO L.F., *Time-frequency analysis of postural sway*, Journal of Biomechanics, Vol. 28, 1995, pp. 603–607.
- [7] WELCH P.D., *The use of fast Fourier transform for the estimation of power spectra: a method based on time averaging over short, modified periodograms*, IEEE Transactions on Audio Electroacoustics, 1967, Vol. AU-15, pp. 70–73.
- [8] COEN L., *Time-frequency analysis*, Prentice Hall Signal Processing Series, 1995.